

## **Computation Design to Simulate an Objective Magnetic Lens and Study of Effect the Distance Between Pole pieces on its Optical Properties**

Mardeen J. AHMED<sup>1</sup> & Mohammed A. HUSSEIN<sup>2</sup>

### **Keywords**

electron microscope, objective magnetic lens, distance between pole piece.

### **Abstract**

In this article, an objective magnetic lens was developed and its optical properties were analysed using simulation programs depending on finite elements method. Better optical properties, low values of electron probe diameter( $d_p$ ) incident on specimen surface, spherical aberration ( $d_s$ ), chromatic aberration ( $d_c$ ), diffraction aberration ( $d_d$ ), Gaussian aberration ( $d_g$ ) and suitable aperture angle ( $\alpha$ ) were achieved. Asymmetric double pole piece magnetic lens with good properties was designed. The effect of the different distances between pole pieces ( $S=2,4,6,8$ )mm, on the magnetic lens properties to achieve the best configuration for the lens was investigated. The results show that at constant excitation ( $NI=1$  kA-t) and acceleration voltage ( $V_r=10$  kV), distance ( $S=2$  mm) was offered good optical properties; focal length ( $f_o=4.04$  mm), spherical aberration ( $C_s=3.75$  mm), chromatic aberration ( $C_c=3.12$  mm). The greatest axial magnetic flux ( $B_z=0.18$  T) was obtained. The diameter of an electron probe as a function of aperture angle was investigated. According to the findings, an aperture angle of ( $=2$  mrad) has improved optical properties ( $d_p=12.24$  mm), ( $d_s=5.64$  mm), ( $d_c=0.0005$  mm), ( $d_d=4.06$  mm), and ( $d_g=10.06$  mm). The L1 design was selected as the best design, and its optical properties were also investigated.

### **Article History**

Received  
19 May, 2022  
Accepted  
30 Dec, 2022

## **1. Introduction**

As the feature sizes of semiconductor devices continue to shrink, scanning electron beam tools experience a growing difficulty due to their comparatively poor utilization: the amount of pixels to be inspected on a wafer results in examination times that surpass realistic limits(1). The scanning electron microscope, which uses an electron beam with a short wavelength less than 1nm(2), is one of the most widely used instruments for measuring and analysing microstructures with high precision. Scanning electron microscopes are classified into two categories based on the kind of electron gun used, namely scanning electron microscopes with field emission and scanning electron microscopes with thermal emission. High analytical capacity tends to use a scanning electron microscope with field emission,

<sup>1</sup> Corresponding Author. ORCID: 0000-0002-2229-106X. University of Kirkuk, College of Science, Department of Physics, mardeenjihad@uokirkuk.edu.iq

<sup>2</sup> ORCID: 0000-0002-5402-9728. University of Kirkuk, College of Education/Al-Hawija, Department of Physics, mohdphy@uokirkuk.edu.iq

however due to the high cost and the need of a high degree of vacuum up to Torr $10^{-10}$ (3,4). In addition to requiring high precision alignment, a thermal emission is recommended for use, and still has a wide market share owing to its low cost and the fact that it needs a low degree of vacuum up to  $10^{-7}$  Torr.

Presently, a scanning electron microscope with a thermal emission that has been used to analyse 50 times greater than the boundary principle as a result of anomalies in the size of electron source, energy dispersive and aberrations across the optical column, and the adoption of accuracy in magnetic lenses, as well as other defects in the processing and engineering field, as a result, manufacturers have based electron microscopes current invention source the electron beam for the degree of high light, machine lenses with low aberration, and scattering a small amount of radiation. Using a scanning electron microscope, an electron beam of a very small wavelength less than 0.01nm is accelerated to improve resolving power in comparison to an optical microscope, which relies on the visible light source wavelength spectrum between 300-700nm(5).

To promote the design of the electron lens system and minimize the time and loss associated with the manufacture of these lenses, as well as to demonstrate their failure, numerical simulation software has been commonly used, as indicated by Munro (4), The electron lens is examined using the finite element method of the first order(6).created analysis programs for electron guns based on the boundary element method. In the other hand, for the study of various types of electron guns (7). Zhu and Munro finite element system of second order was used (8).used the Monte Carlo method to quantify the scattered electrons. In the configuration of the spectroscopy scanning electron microscope, utilizing the finite element methods (3).

The objective lens had been Consider the essential electron microscope components that make on the focus of the falling electron beam on the specimen surface and defines the amount of inspection of the instrument for being the only element that greatly contributes to reducing the size of Spherical Cs and chromatic Cc aberrations in the optical column that strongly deflects electrons in the direction of the optical axis. To reduce spherical Cs and chromatic Cc aberrations, position the sample at the peak of the magnetic fields near the magnetic poles of the objective lens (9).Objective magnetic lens of the from type Pinhole can be designed and investigate the electromagnetic properties described by the distribution of the axial magnetic flux density  $B_z$  and the direction of the electron beam at various acceleration voltages, as well as the path of magnetic flux lines within the lens, as well as the measurement of optical properties such as Spherical Cs and chromatic Cc aberration coefficients and focal length  $f_o$  to obtain sufficient objective lens properties for use in a scanning electron microscope(10).The spherical and chromatic aberration coefficients in the electron microscope are known to be greater where the strength of the lens field is greater near the specimen and the focal length is smaller. As a result, it is common to choose that the specimen be mounted near the center of the lens. However, in order to use the lens feature more effectively, the specimen has been selected or mounted on the side of the electron source with respect to the central of the lens that focuses the image of the specimen(11). When the interior of the lens is produced vacuum,

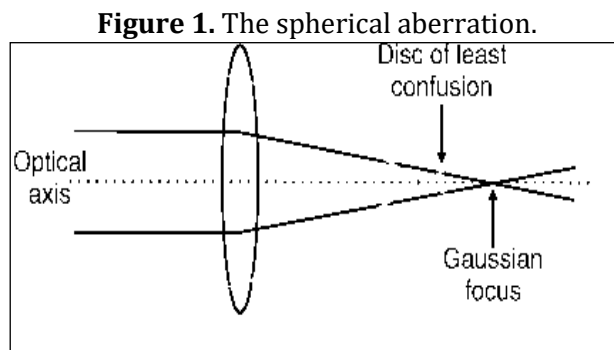
however, the focal length is always reduced due to spherical aberration, and the crossover of the off-axial electron beams is always closer to the electron source than that of the paraxial beams. The distance between them grows at a rate equal to the cube of the distance between the beam and the axes. As a result, the spherical and chromatic aberration coefficients will be reduced if the specimen is positioned in the middle of the lens, a combination occurs between the off-axial beams which penetrate the center of the specimen and the paraxial beams. As a result of the massive aberration, the image becomes obscure, requiring the use of a very narrow aperture for a transparent image. However, such a narrow aperture limits the optical range and creates difficulties in producing and maintaining the aperture, making it unsuitable for practical use (12).

The electrons pass far away from the optical axis of the lens are more strongly deflected than those whose nearly passed as shown figure 1. It can be noticed that the Disk of Least Confusion (ds) of spherical aberration given in equation 1 is produced due to non-intersect rays at one point(13).

$$ds = 0.5C_s \alpha^3 \tag{1}$$

Where,  $C_s$  and  $\alpha$  are spherical aberration and angle of aperture respectively.

One of the important aberration occur in the objective lenses which is used to determine the resolving power in electron microscope is the spherical aberration because it effects the quality of produced image(14).



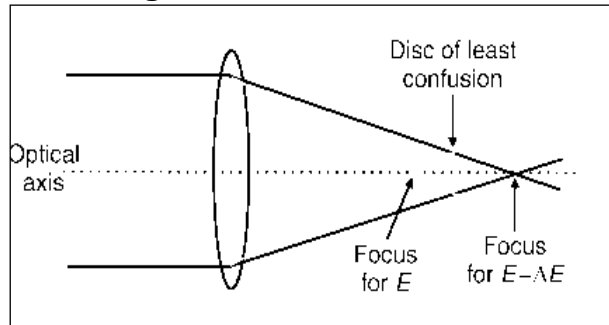
The velocity differences of the emitted electrons from the electron gun due to the difference in the electron energy make them to intersect with optical axis at two different points which leads to produce the Disk of Least Confusion ( $d_c$ ) of chromatic aberration ( $C_c$ ) illustrated in figure 2 below . The Disk of Least Confusion ( $d_c$ ) can be given by:

$$d_c = C_c \frac{\Delta E}{E} \alpha \tag{2}$$

Where,  $C_c$  is the chromatic aberration,  $\Delta E$  is the extension energy at the gun,  $E$  is acceleration beam energy and  $\alpha$  is the angle of aperture.

The chromatic aberration can be reduced by increasing the energy of acceleration beam and using a small diameter of aperture.

**Figure 2: Chromatic aberration**



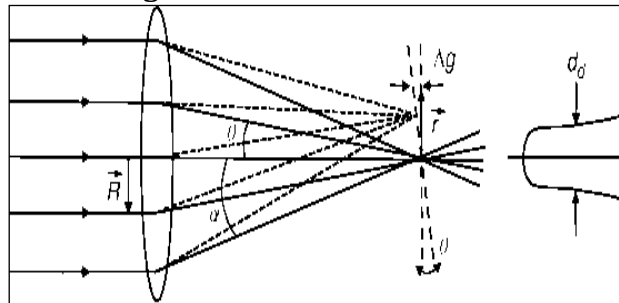
According to the wave nature of electron beam, the beam deflects from its path behind the small aperture. As a result, the electron beam will extend then the airy disc will be appeared due to Fraunhofer diffraction, see figure 3 (15). The diffraction aberration ( $d_d$ ) is given by:

$$d_d = \frac{0.61\lambda}{\alpha} \quad (3)$$

Where,  $\lambda$  is de Broglie wavelength and  $\alpha$  is the angle of aperture.

By equation 3 can be seen that the  $d_d$  is inversely proportional to  $\alpha$  while  $d_c$  and  $d_s$  are both proportional to  $\alpha$  see equations (1,2), as a result,  $d_d$  is inversely proportional to  $d_c$  and  $d_s$ . The angle of aperture is determined by chromatic and spherical aberrations in the range of several millirads (mrad), while, the contribution of diffraction aberration is in the range of several nanometers (nm) (13).

**Figure 3. Diffraction aberration.**



## 2. Methodology

In this paper, changes of the distance between of pole piece to get on clear image of specimen surface by reduce the aberrations and demagnification of the electron probe diameter.

Resolving power of a few parts from micrometer was obtained in the conventional scanning electron microscope By using very small working distances and high acceleration voltage (more than 20 kV), As results, destruction for the conductive specimens or Integrated circuits will occur, because of a high acceleration voltage. Therefore, Recent research started to focus on an attempt to obtain of high analysis of specimen surface at relatively low acceleration voltages (less than 20

kV), particularly at Examination of semiconductor specimens by a scanning electron microscope (16).

Extensive studies were conducted to improve the geometrical shape of the magnetic lens, these studies confirmed that each parameter of the lens parameters; distance between pole pieces, shape the pole piece, dimensions of lens, dimensions of coil, location of coil, etc. it all have relatively important from both respects of practical and theoretical to obtain at clear image in the scanning electron microscope.

### 3. Results and discussion

Figure 4 shows four designs of equal dimensions of magnetic lens. Different distances between polepieces ( $S=2,4,6,8$ ) mm were used in designing the lenses at a constant dimensions. For clarification, the inner and outer diameters of the lens are about 5 mm and 65 mm respectively, the lens length is 55 mm and the dimensions of the lens coil are (30×30) mm for all lenses which designed. The colors (blue, red and green) represent respectively; coil, polepiece and the Yoke.

**Figure 4.** Four designs of equal dimensions of objective magnetic lens with Different distance between polepieces ( $S=2,4,6,8$ ) mm

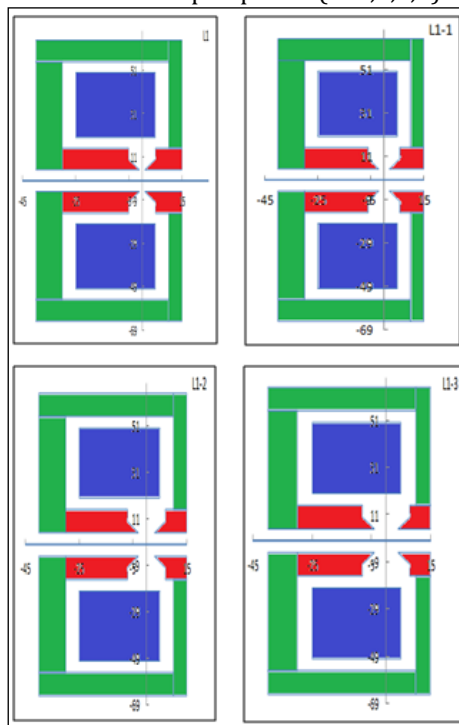


Figure 5 clarify the distribution of axial magnetic flux density ( $B_z$ ) at constant lens excitation ( $NI= 1 \text{ kA-t}$ ) as a function of optical axis ( $Z$ ). It can be noticed that the highest magnetic flux density at the lens (L1) was achieved when the distance between polepieces is equal to (2 mm), while, the flux is lowest at the lens (L1-3) which has a distance of (8 mm).

**Figure 5.** The axial magnetic flux density distribution ( $B_z$ ) for all four designs at a constant lens excitation ( $NI= 1 \text{ kA-t}$ ).

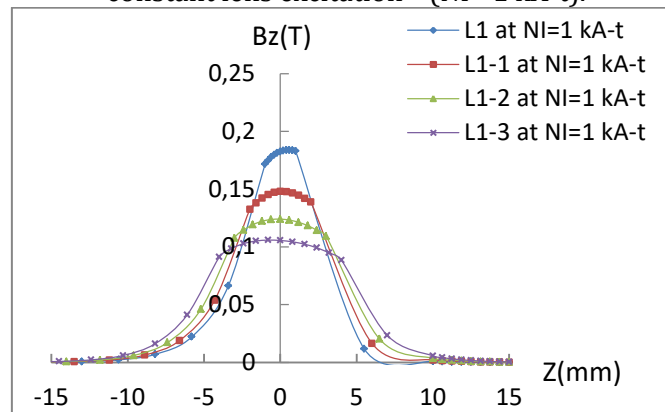


Figure 6 shows change the focal properties; focal length ( $f_o$ ), spherical aberration ( $C_s$ ) and chromatic aberration ( $C_c$ ) as a function of distance between polepieces ( $S$ ) of lenses at a constant excitation ( $NI= 1 \text{ kA-t}$ ) and acceleration voltage ( $V_r= 10 \text{ kV}$ ) for lenses. It can be observed that the lens which has distance of 2 mm it achieved lowest focal length (4.04 mm), spherical aberration (3.75 mm) and chromatic aberration (3.12 mm).

**Figure 6.** The focal length and aberration of four lenses.

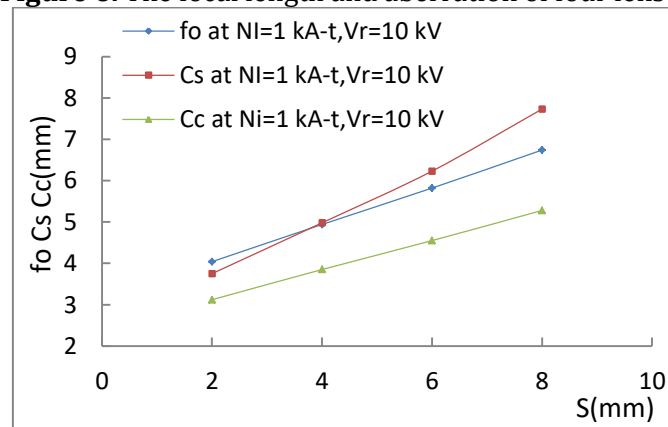


Figure 7 illustrate the distribution of axial magnetic flux density ( $B_z$ ) at different lens excitations ( $NI= 1, 1.25, 1.5, 1.75$ ) kA-t as a function of optical axis ( $Z$ ) for a chosen lens (L1). As shown in the figure, the highest magnetic flux density of (0.32 T) was obtained when the lens excitation equal to (1.75 kA-t), while, it is lowest of (0.18 T) at (1 kA-t). For the selected lens, it is revealed that having a high excitation gives a low aberrations and low focal length. As a results, a clear image will be obtained for the specimen.

**Figure 7.** The axial magnetic flux density distribution ( $B_z$ ) for the selected lens at different lens excitations ( $NI= 1, 1.25, 1.5, 1.75$ ) kA-t.

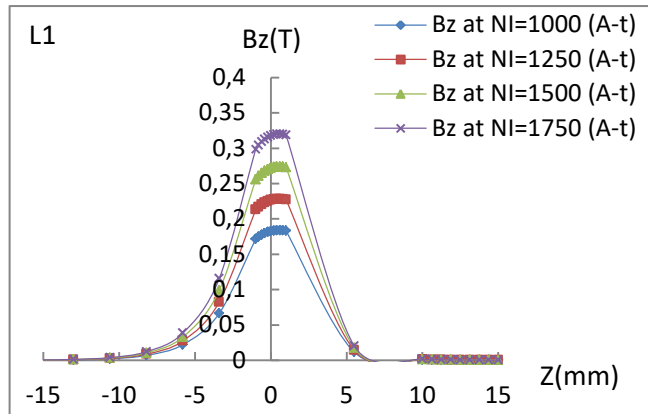


Figure 8 shows the relation between the optical properties; focal length, spherical aberration, chromatic aberration and the excitation parameter ( $NI/\text{SQRT}(V_r)$ ) at a constant lens excitation of 1.75 kA-t. For this excitation, it can be seen that all optical properties ( $f_o$ ,  $C_s$ , and  $C_c$ ) have gradually decreased when the excitation parameter has increased.

**Figure 8.** The relation between the optical properties and the excitation parameter of chosen lens.

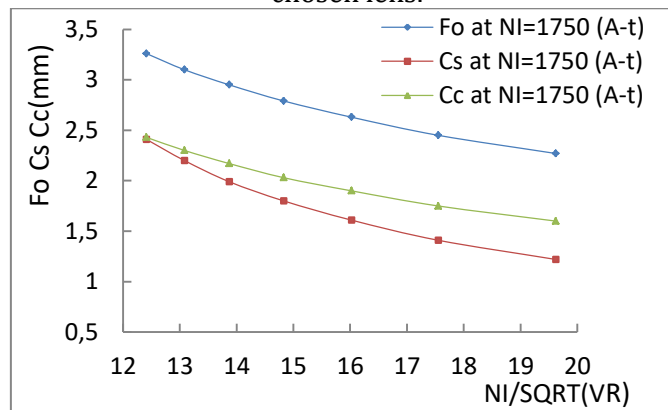
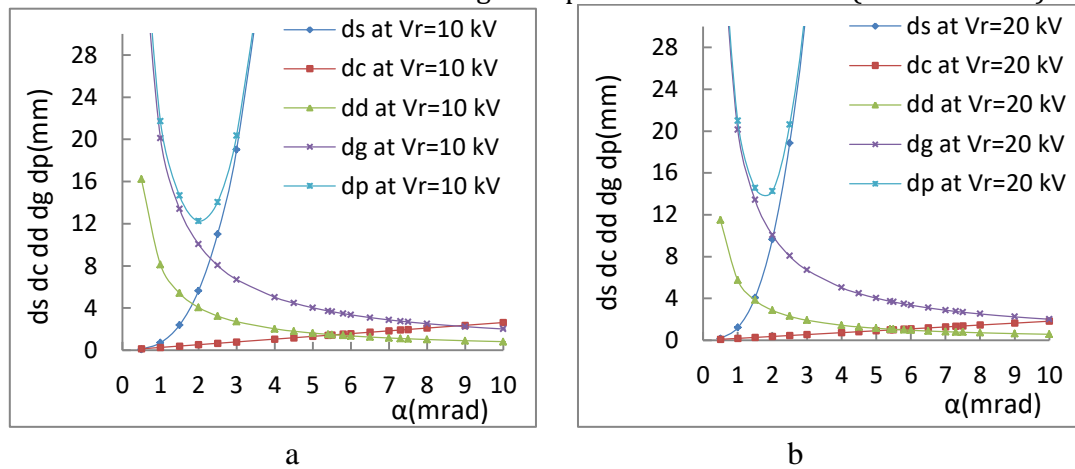


Figure 9 illustrate the relationship between the diameter of electron probe ( $d_p$ ) and magnetic lens aberrations as a function of aperture angle ( $\alpha$ ) at lens excitation ( $NI = 1.75$  kA-t), we note from the figure that the Spherical aberration  $C_s$ , chromatic aberration  $C_c$  decrease when reducing the value of aperture angle ( $\alpha$ ), while, diffraction aberration  $d_d$  was increasing. Therefore, suitable aperture angle was existed that gives least aberrations and minimum probe diameter. From figure 9a better properties ( $d_s=5.64$  mm),( $d_c=0.52$  mm),( $d_d=4.06$  mm),( $d_g=10.06$  mm),( $d_p=12.24$  nm) were achieved at angle of aperture (2 mrad).

**Figure 9.** Shows the relationship between the electron probe diameter and magnetic lens aberrations as a function to the angle of aperture  $\alpha$  at excitation ( $NI = 1.75 \text{ kA-t}$ )



#### 4. Conclusions

The current study was revealed that the distance between the polepieces has a clear effect on the optical properties of the magnetic lens, good results were achieved at distance of 2 mm for optical properties; magnetic flux density, spherical and chromatic aberrations, focal length and diameter of the electron probe. In addition, the aperture angle has great importance in determining the resolving power by determining the minimum diameter of the electron probe which gives the least aberration. Aperture angle of 2 mrad gave a smaller diameter of the electron probe and thus less aberrations.

#### References

1. Mankos M, Adler D, Veneklasen L, Munro E. Electron optics for low energy electron microscopy. *Phys Procedia*. 2008;1(1):485–504.
2. Khursheed A. Magnetic axial field measurements on a high resolution miniature scanning electron microscope. *Rev Sci Instrum*. 2000;71(4):1712–5.
3. Joseph Goldstein, Dale E. Newbury, David C. Joy, Charles E. Lyman, Patrick Echlin, Eric Lifshin, Linda Sawyer JRM. *Scanning Electron Microscopy and X-ray Microanalysis: Third Edition*. 2012;690.
4. Hayward AF. Book Review. *J Dent*. 1973;2(1):46–7.
5. Peter Hawkes EK. *Principles of Electron Optics*. Principles of Electron Optics. 2018.
6. Hussein MA. Effect of the Geometrical Shape of the Magnetic Poles and the Distance between Them on the Focal Properties of the Condenser Magnetic Lens in the Scanning Electron Microscope ( SEM ). 2016;4(5):130–4.



7. Park MJ, Park K, Kim DH, Jang DY. Design and analysis of a thermionic SEM column using 3D finite element analysis. *Phys Procedia*. 2008;1(1):199–205.
8. Azad M, Avin A. Scanning Electron Microscopy (SEM): A Review. *Proc 2018 Int Conf Hydraul Pneum - HERVEX*. 2019;(January):1–9.
9. Hussein MA. Estimating electron probe diameter in the scanning electron microscope. 2016;6(18):68–73.
10. Abbas TM. Correction of Distortion Aberration in Electron Magnetic Lenses. *Int J Appl Phys*. 2016;3(3):1–4.
11. Numan NH. Theoretical Study of Geometrical Properties and Aberrations in Doublet Magnet Lenses. 2018;(26):178–87.
12. DeWitt H. Objective Lens. *Fine Focus*. 2019;5(1):5–13.
13. Stokes DJ. Principles and Practice of Variable Pressure/Environmental Scanning Electron Microscopy (VP-ESEM). *Principles and Practice of Variable Pressure/Environmental Scanning Electron Microscopy (VP-ESEM)*. 2008. 1–221 p.
14. Bell DC, Erdman N, Brooks S. *Low Voltage Electron Microscopy: Principles and Applications*. Low Voltage Electron Microscopy: Principles and Applications. 2012.
15. Stephen J. Pennycook (auth.), Stephen J. Pennycook PDN (eds. . *Scanning Transmission Electron Microscopy Imaging and Analysis*. Pennycook SJ, Technology MS and, editors. USA; 2011. 755 p.
16. David M. ( 12 ) Patent Application Publication ( 10 ) Pub . No .: US 2017 / 0215756A1. 2017;1(19):2015–8.

---

© Copyright of Journal of Current Researches on Educational Studies is the property of Strategic Research Academy and its content may not be copied or emailed to multiple sites or posted to a listserv without the copyright holder's express written permission. However, users may print, download, or email articles for individual use.